THE JOURNAL OF PHYSICAL CHEMISTRY B

Article

Cite This: J. Phys. Chem. B 2018, 122, 10362−10370

pubs.acs.org/JPCB

Does α-Tocopherol Flip-Flop Help to Protect Membranes Against Oxidation?

Published as part of The Journal of Physical Chemistry virtual special issue "Deciphering Molecular Complexity in Dynamics and Kinetics from the Single Molecule to the Single Cell Level".

Phansiri Boonnoy,[†,‡] Mikko Karttunen,[*,§,∥] and Jirasak Wong-ekkabut[*,†,‡,⊥,#]

[†]Department of Physics, Faculty of Science, [‡]Computational Biomodelling Laboratory for Agricultural Science and Technology, Faculty of Science, and [#]Specialized Center of Rubber and Polymer Materials for Agriculture and Industry, Faculty of Science, Kasetsart University, Bangkok 10900, Thailand

[§]Department of Chemistry and [∥]Department of Applied Mathematics, Western University, 1151 Richmond Street, London, Ontario N6A 5B7, Canada

[⊥]Thailand Center of Excellence in Physics, Commission on Higher Education, Bangkok 10400, Thailand

Supporting Information

ABSTRACT: α-Tocopherols (α-toc) are crucial in protecting biological membranes against oxidation by free radicals. We investigate the behavior of α-toc molecules in lipid bilayers containing oxidized lipids by molecular dynamics (MD) simulations. To verify the approach, the location and orientation of α-toc are first shown to be in agreement with previous experimental results. The simulations further show that α-toc molecules stay inside the lipid bilayer with their hydroxyl groups in contact with the bilayer surface. Interestingly, interbilayer α-toc flip-flop was observed in both oxidized and nonoxidized bilayers with significantly higher frequency in aldehyde lipid bilayer. Free-energy calculations were performed, and estimates of the flip-flop rates across the bilayers were determined. As the main finding, our results show that the presence of oxidized lipids leads to a significant decrease of free-energy barriers and that the flip-flop rates depend on the type of oxidized lipid present. Our results suggest that α-toc molecules could potentially act as high-efficacy scavengers of free radicals to protect membranes from oxidative attack and help stabilize them under oxidative stress.

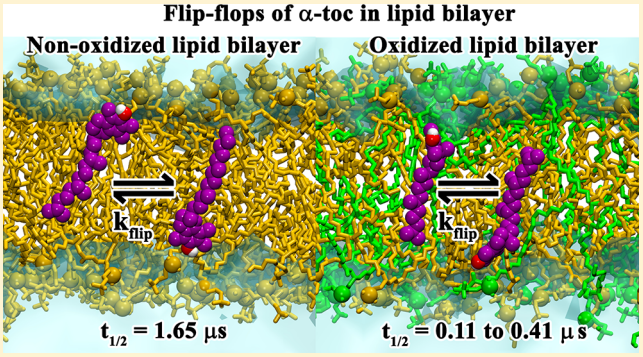

INTRODUCTION

An imbalance between the production and elimination of oxidizing lipid species in cell membrane can lead to oxidative attack on unsaturated lipids.[1] α-Tocopherol (α-toc; a form of vitamin E) is the most abundant and important lipophilic antioxidant found in cell membranes.[2−4] It is known to act as an essential radical scavenger protecting membranes from oxidation, but several key aspects of the molecular mechanisms of this action remain uncovered. α-toc inhibits lipid peroxidation process by donating a hydrogen atom to a lipid-peroxyl radical and becoming an α-tocopheroxyl radical.[5] Although chemical assessment of α-toc's antioxidant ability has been shown, the mechanisms by which it stabilizes membranes are debated.[3,6−9]

Significant experimental and computational effort has been invested in characterizing the location and interactions of α-toc in model membranes,[8−19] but obtaining precise information has proven to be challenging,[9,16] and the behavior and interaction mechanisms of α-toc molecules inside an oxidized lipid bilayer are being debated. Biophysical studies have, however, demonstrated that the chromanol ring of α-toc is located at the lipid−water interface.[12,13,16] This suggests that membrane surface is the key to α-toc's antioxidant activity. It has also been suggested that α-toc partitions in membrane regions are rich in polyunsaturated lipids, but more studies are needed to confirm this.[8,9]

In addition to the above, molecular dynamics (MD) simulations at elevated temperatures have demonstrated the presence of transmembrane flip-flops.[10,11] It has been shown that the flip-flop rate depends on temperature, the degree of unsaturated lipid chains, and the fluidity of the lipid membrane.[10,11] It has been shown that flip-flops are intimately related to trapping free radicals near the lipid−water interface allowing for the lipid peroxyl radical(s) to be removed.[16] However, thus far there is no information on how α-toc behaves after lipid peroxidation has occurred. In addition, the

Received: September 16, 2018
Revised: October 14, 2018
Published: October 24, 2018

DOI: 10.1021/acs.jpcb.8b09064
J. Phys. Chem. B 2018, 122, 10362−10370

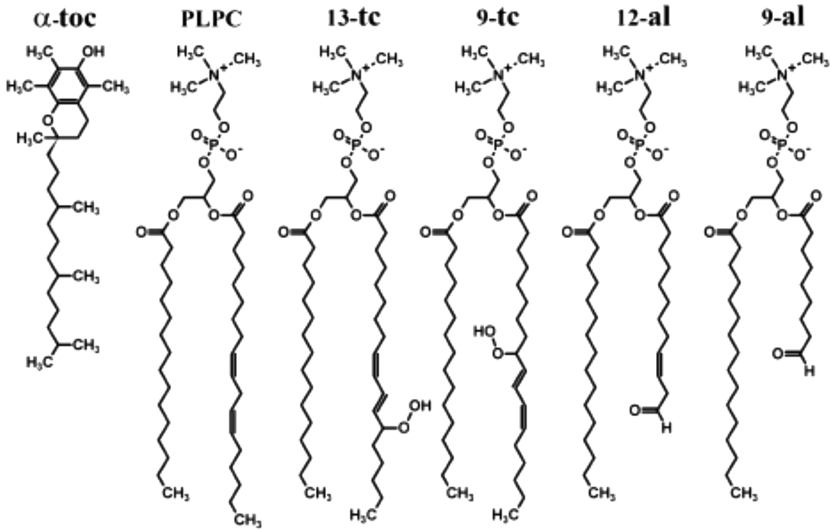

Figure 1. Chemical structures of the α-toc and lipid molecules. (left to right) α-toc, PLPC, 13-tc, 9-tc, 12-al, and 9-al.

functions and molecular insight into α-toc's actions in oxidative cell membrane remain unclear. In our previous MD simulations[18] we have shown that α-toc inhibits pore formation in oxidized lipid bilayers. In particular, α-tocs help to stabilize the bilayer structure by trapping the polar oxidized functional group at the water interface thus reducing water permeability across the bilayer. In addition, transmembrane flip-flop of α-toc were observed in both oxidized and nonoxidized bilayer even at room temperature. However, the energetics of the process need to be elaborated.

In this work, we focus on the dynamics and kinetics of α-toc flip-flop in both pure and oxidized lipid bilayers. The effects of different oxidized functional groups were studied. The free-energy profiles for α-toc desorbing out of the bilayer were calculated, and the flip-flop rates were estimated. The results show that the free-energy barriers become significantly decreased in the presence of oxidized lipids and that the flip-flop rates depend on the type of oxidized lipid present. This study presents new evidence of how α-toc protects oxidized cell membranes.

METHODOLOGY

We performed MD simulations of oxidized and nonoxidized phospholipid bilayers at various α-toc concentrations. All of the lipid bilayers had 128 lipid molecules (64 per leaflet). A 100% 1-palmitoyl-2-linoleoyl-*sn*-glycero-3-phosphatidylcholine (PLPC) lipid bilayer was used as a reference to characterize the effects of α-toc on a nonoxidized bilayer. For the oxidized bilayers, we used 1:1 binary mixtures of PLPC and its four main oxidative derivative products, namely, two hydroperoxides (1-palmitoyl-2-(9-hydroperoxytrans-10, cis-12-octadecadienoyl)-*sn*-glycero-3-phosphocholine, 9-tc and 1-palmitoyl-2-(13-hydroperoxy-trans-11,cis-9-octadecadienoyl)-*sn*-glycero-3-phosphocholine, 13-tc), and two aldehydes (1-palmitoyl-2-(9-oxo-nonanoyl)-*sn*-glycero-3-phosphocholine, 9-al and 1-palmitoyl-2-(12-oxo-cis-9-dodecenoyl)-*sn*-glycero-3-phosphocholine, 12-al). The molecular structures of α-toc and the lipids are shown in Figure 1. We studied bilayers with 0, 2, 4, 8, and 16 α-toc molecules (equivalent to the concentrations of 0%, 1.5%, 3.0%, 5.9%, 11.1%, respectively). All systems were solvated in 10 628 simple point charged (SPC) water.[20] The parameters of both PLPC and the oxidized lipids were taken from previous studies.[21−23] Detailed descriptions of the topologies and force-field parameters of α-toc are provided in refs 10 and 11. Initially, α-toc molecules were randomly placed in the water phase at ∼4.2 nm in the z-direction from the center of the bilayer. The passive penetration times of the α-toc molecules into the bilayers varied from tens to several hundreds of nanoseconds. At the high concentrations (5.9% and 11.1%) α-toc molecules required much longer times to enter the lipid bilayer (over several microseconds), and in some cases pore formation occurred before complete translocation of α-toc molecules into the lipid bilayer. To avoid artificial pore formation induced by the initial conditions, the α-toc molecules were randomly inserted at the lipid−water interface at high concentrations. The details of all simulations are provided in Table 1.

Simulation Details. After energy minimization using the steeped descents algorithm, MD simulations were run for 1−5 μs with 2 fs integration time step using the GROMACS 5.1.1 package.[24] All simulations were performed in the constant of particle number, pressure, and temperature (NPT) ensemble. The v-rescale algorithm[25] at 298 K with a time constant of 0.1 ps was used for temperature control, and equilibrium semi-isotropic pressure was set at 1 bar using the Parrinello−Rahman algorithm[26] with a time constant of 4.0 ps and compressibility of 4.5×10^{-5} bar^{-1}. Periodic boundary conditions were applied in all directions, and the neighbor list was updated at every time step. A cutoff of 1.0 nm was applied for the real space part of electrostatic interactions and Lennard-Jones interactions. The particle-mesh Ewald method[27−29] was used to compute the long-range part of electrostatic interactions with a 0.12 nm grid in the reciprocal-space interactions and cubic interpolation of order four. All bond lengths were constrained by the P-LINCS algorithm.[30] The optimized parameters and protocols have been extensively tested and used previously, for example, in refs 18,23, and 31−33. All visualizations were done using Visual Molecular Dynamics (VMD) software.[34]

Free-Energy Calculations. The umbrella sampling technique[35] with the Weighted Histogram Analysis Method[36] (WHAM) was used to calculate the potential of mean force (PMF) for transferring an α-toc through the 100% PLPC, 50% 13-tc, 50% 9-tc, 50% 12-al, and 50% 9-al bilayers. For each

DOI: 10.1021/acs.jpcb.8b09064
J. Phys. Chem. B 2018, 122, 10362−10370

Table 1. List of Systems Studied Here

No.	description of the systems	simulation time (ns)	final structure
1	100% PLPC	1000	bilayer
2	100% PLPC + 2 α-toc (1.5%)	1000	bilayer
3	100% PLPC + 4 α-toc (3.0%)	1000	bilayer
4	100% PLPC + 8 α-toc (5.9%)	1000	bilayer
5	50% 13-tc	1000	bilayer
6	50% 13-tc +2 α-toc (1.5%)	1000	bilayer
7	50% 13-tc +4 α-toc (3.0%)	1000	bilayer
8	50% 13-tc +8 α-toc (5.9%)	1000	bilayer
9	50% 9-tc	1000	bilayer
10	50% 9-tc +2 α-toc (1.5%)	1000	bilayer
11	50% 9-tc +4 α-toc (3.0%)	1000	bilayer
12	50% 9-tc +8 α-toc (5.9%)	1000	bilayer
13	50% 12-al	1000	bilayer with a pore (576 ns)
14	50% 12-al +2 α-toc (1.5%)	1500	bilayer with a pore (1064 ns)
15	50% 12-al +4 α-toc (3.0%)	3000	bilayer with a pore (2802 ns)
16	50% 12-al +8 α-toc (5.9%)	4000	bilayer with a pore (3394 ns)
17	50% 12-al +16 α-toc (11.1%)	5000	bilayer
18	50% 9-al	1000	bilayer with a pore (577 ns)
19	50% 9-al +2 α-toc (1.5%)	1000	bilayer with a pore (391 ns)
20	50% 9-al +4 α-toc (3.0%)	5000	bilayer with a pore (4794 ns)
21	50% 9-al +8 α-toc (5.9%)	2000	bilayer with a pore (1589 ns)
22	50% 9-al +16 α-toc (11.1%)	5000	bilayer

[a]Each 100% PLPC bilayer and 50% hydroperoxide (13-tc, 9-tc) mixture was run for 1 μs. The 50% aldehyde (12-al, 9-al) mixtures were run for 1−5 μs to study the effects of α-toc on pore formation. Pore formation time and when a pore/pores occurred is shown in the brackets in the column marked final structure. Both the absolute number and the percentage of α-toc molecules are given in the column description of the system.

system, a series of 41 simulation windows was run to compute the PMF profile as a function of the distance between α-toc and the bilayer center varying from z = 0 nm (bilayer center) to z = 4.0 nm (water phase) with 0.1 nm increments. A harmonic potential was applied between the center of mass of the bilayer and the α-toc hydroxyl group with a harmonic force constant of 3000 kJ/(mol nm^2). Each window was run in the NPT ensemble at 298 K for at least 50 ns; the total time of each PMF profile was at least 2.05 μs. The last 20 ns was used for analysis. The statistical uncertainty in umbrella sampling simulations was estimated by the bootstrap analysis method.[37]

RESULTS AND DISCUSSION

A series of MD simulations of α-toc molecules in different lipid bilayers was performed to study their dynamics in both oxidized and nonoxidized bilayers. Previous MD simulations[18] have shown that the presence of ∼6%−11% of α-toc molecules in an aldehyde bilayer helps protect against passive pore formation induced by oxidized lipids.[38] In this work, pore formation was observed in aldehyde bilayers at 5.9% of α-toc, but the time to form a pore extended for over 1−3 μs. We confirmed that 11.1% α-toc in aldehyde bilayers can prevent pore formation and help to stabilize the oxidized bilayer for times exceeding 5 μs (Figure 2A,B). Interestingly, MD simulations also showed that α-toc's orientations and transmembrane flip-flops are different in nonoxidized and oxidized bilayer. This indicates that the interactions of α-toc with the bilayer are different before and after lipid peroxidation. It may also indicate, although it must be tested by experiments, that these differences are important in determining α-toc's antioxidant action. To characterize the flip-flops, we calculated the free-energy profiles for α-toc desorbing out of the bilayer and estimated the rate of α-toc flip-flop. These issues will be discussed below.

The Behavior of α-toc inside the Lipid Bilayers. To investigate where α-toc molecules reside inside the different bilayers, we investigated the time evolution of the positions of α-tocs' hydroxyl groups along the z-axis (Figure 3). The results show the hydroxyl groups prefer to stay at the bilayer-water interface around the carbonyl group (see Figure 1 for the lipid structures) for both oxidized and nonoxidized bilayers, Table S1. This is in agreement with previous MD simulations[18] and experiments.[9]

In nonoxidized membranes, the presence of α-toc molecules in the lipid−water interface region helps to protect the bilayer from approaching free radicals.[5] When oxidized lipids are present, α-toc flip-flop has an important function in helping to reach and scavenge peroxyl radicals within the lipid bilayer.[16] Figure 2C−G shows snapshots of α-toc transmembrane flip-flop. In the next two sections we quantified the process by computing the free energy and the flip-flop rates, but as an indicative rough comparison we followed the molecules in five lipid bilayers containing 5.9% α-toc molecules over 1 μs and found 21, 10, 16, 7, and 4 events for 50% 9-al, 50% 12-al, 50% 13-tc, 30% 9-tc, and 100% PLPC lipid bilayers, respectively. For the aldehyde bilayers containing 11.1% α-toc molecules, we observed 136 flip-flops for the 50% 9-al bilayer and 162 for the 50% 12-al bilayer over 5 μs. This suggests that the faster dynamics of the α-toc molecules may be a key to its antioxidant action and consequent stabilization of the bilayer under oxidative stress.

The orientations of the α-toc molecules were investigated by calculating the angle between the bilayer normal (z-axis) and a vector connecting the last methyl group in the tail to the hydroxyl group in the headgroup (see Figure 1 for the molecular structures). The last 500 ns (before pore creation in aldehyde bilayers) of lipid bilayers with 5.9% α-toc molecules were used for analysis and shown in Figure 4 and Figure S1. The angles range between 0 and 90°: 0° is equal to alignment parallel to the bilayer normal, and 90° corresponds to being perpendicular to the bilayer normal. To check the generality of this approach, we also calculated the orientations of the α-toc molecules by using the vector connecting the weight center of the tail to the hydroxyl group in the headgroup of α-toc molecules. Both methods yield full consistent distributions for the tilt angle as shown in Figure S2. For the PLPC lipid bilayer, most of the α-toc's hydroxyl groups were found to be located slightly underneath the lipids' carbonyl groups within the lipid bilayer (Table S1) in agreement with previous experimental

DOI: 10.1021/acs.jpcb.8b09064
J. Phys. Chem. B 2018, 122, 10362−10370

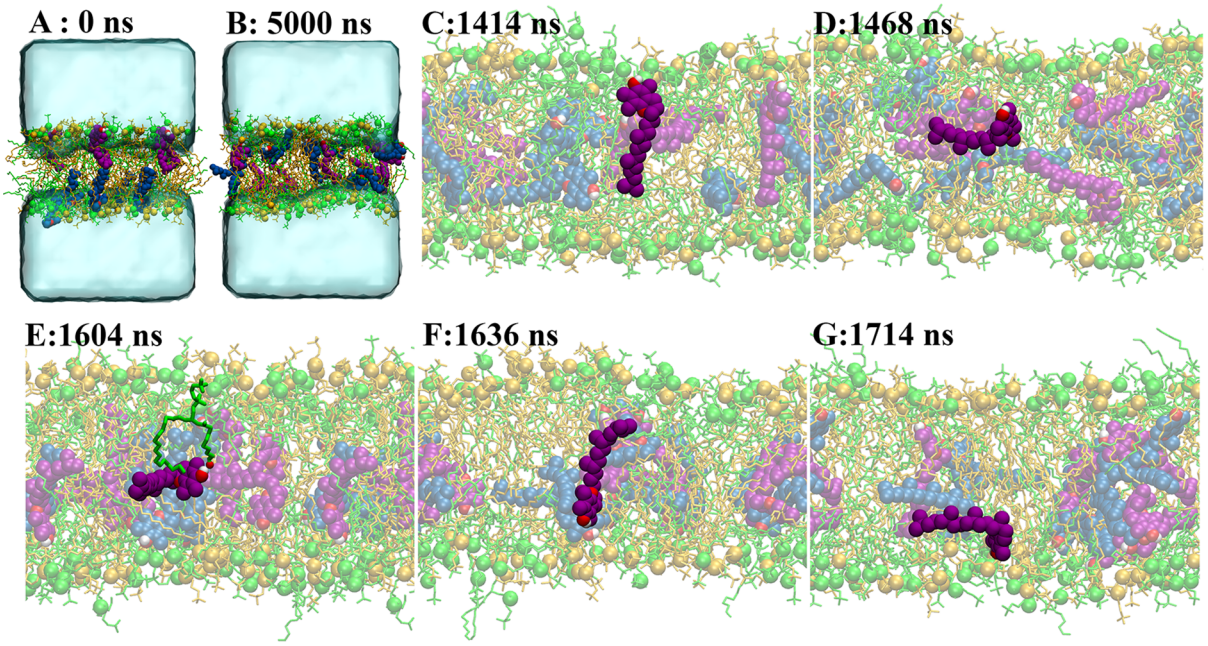

Figure 2. α-toc flip-flop in a 50% 9-al bilayer with 11.1% α-toc molecules present. (A) Initial structure at 0 ns. The 16 α-toc molecules were randomly inserted at the lipid−water interface (eight molecules in each leaflet). PLPC and 9-al lipids are shown as yellow and green lines, respectively, with phosphorus atoms as spheres. α-toc molecules are shown in purple and blue spheres, which represent α-tocs in the upper and lower leaflets, respectively. Water is shown in light blue (only in (A) for clarity). Oxygen and hydrogen atoms of the α-toc molecules are shown in red and white spheres, respectively. (B) The final structure at 5 μs (A) shows that α-tocs have moved (via flip-flop) between the two leaflets. (C−E) The α-toc molecule reorients itself to move toward the bilayer center. Within the aldehyde oxidized bilayer, α-toc's hydroxyl group can form a hydrogen bond with the oxidized lipid tail (E) leading to an increase in the flip-flop rate in the oxidized bilayer. Reorientation of α-toc molecules was observed when they moved to the lower leaflet with the hydroxyl group facing the lipid headgroup and the hydrophobic tail randomly spreading within the bilayer (F, G).

studies.[8,9,19] The tilt angles of the α-toc molecules with respect to the bilayer normal are shown in Figure 4A. Two possible orientations at ∼40 ± 12° and 90 ± 4° to the bilayer normal were observed in PLPC bilayer. In contrast to experiments, the chains of α-toc and saturated 1,2-dimyristoyl-*sn*-glycero-3-phosphocholine (DMPC) and 1,2-dipalmitoyl-*sn*-glycero-3-phosphocholine (DPPC) lipids are oriented with the relative angles of 11 ± 2 and 16 ± 4°, respectively, which may imply to the only parallel orientation to the bilayer normal.[19] However, the α-toc tilt angle is still being debated, since discrepancies can arise from differences in lipid types, lipid phase, and location of α-toc inside the bilayer.[10,17,19] In an analogous manner, differences in tilt angle have been shown to indicate the ability of different sterols to undergo flip-flop.[39] For a general discussion of lipid flip-flops, see articles by Gurtovenko and Vattulainen[40] and Sapay, Bennett, and Tieleman.[41]

For the hydroperoxide lipid bilayer, the polar head groups of the α-toc molecules prefer to stay at the bilayer-water interface in a way similar to what is observed for the PLPC bilayer. The average distances of the carbonyl group from the bilayer center are 1.32 ± 0.01 and 1.37 ± 0.02 nm for 50% 13-tc and 50% 9-tc bilayer, respectively. Meanwhile, the locations of the hydroxyl group of α-toc molecules in 50% 13-tc and 50% 9-tc bilayer are 1.03 ± 0.02 and 1.08 ± 0.04 nm from the bilayer center, respectively. However, all α-toc molecules in the hydroperoxide bilayer prefer to be slightly tilted in parallel to the bilayer (tilted angle is ∼40−60° to the bilayer normal) rather than to lie horizontally in the bilayer (Figure 4B,C). For the aldehyde lipid bilayer, a wide range of orientations was observed caused by a random spread of the α-toc's hydrophobic tail in the bilayer (Figure 4D,E). Interestingly, it can be seen a flip-flop typically follows (Figure 4D,E) when the α-toc's hydroxyl moves deep inside the bilayer and reorients. The molecular length ($\vec{l}$) of α-toc in lipid bilayer was determined as the distance between the terminal methyl group in the tail and the hydroxyl group in the head (see Figure 1 for molecular structures). The molecular length distribution of α-toc in nonoxidized/oxidized lipid bilayers is shown in Figure 5. The results show an extended structure in both PLPC and oxidized bilayers with the maximum probability densities in molecular length being ∼2.06 ± 0.01 nm (Figure 5). The average molecular lengths were found to be 1.88 ± 0.02, 1.87 ± 0.01, 1.91 ± 0.01, 1.85 ± 0.01, 1.86 ± 0.01 nm in PLPC and 13-tc, 9-tc, 12-al, and 9-al lipid bilayers, respectively. Note the emergence of a shoulder in the case of 5.9% 12-al (solid blue curve). As Figure 4 shows, pore formation is observed in this system. These structures are maintained even when the α-toc molecules move toward the bilayer center and undergo a flip-flop to the opposite side of the bilayer (Figure 4F−J). Note the shortened structure of α-toc when they tilt away from bilayer as seen in Figure S3.

Free Energy Profile of α-toc Molecule in the Bilayer.

Figure 6 shows the PMF profiles for moving an α-toc molecule from the bilayer center to the water phase, and Table 2 lists the equilibrium positions (corresponding to the α-toc hydroxyl group), the free energy of desorption (ΔG_{desorb}) for moving an α-toc from its equilibrium position in bilayer into bulk water, and the free-energy barrier ($\Delta G_{barrier}$) for moving an α-toc from the equilibrium position to the bilayer center. Note that thermal energy is ∼2 kJ mol^{-1}. These results suggest that the

DOI: 10.1021/acs.jpcb.8b09064
J. Phys. Chem. B 2018, 122, 10362−10370

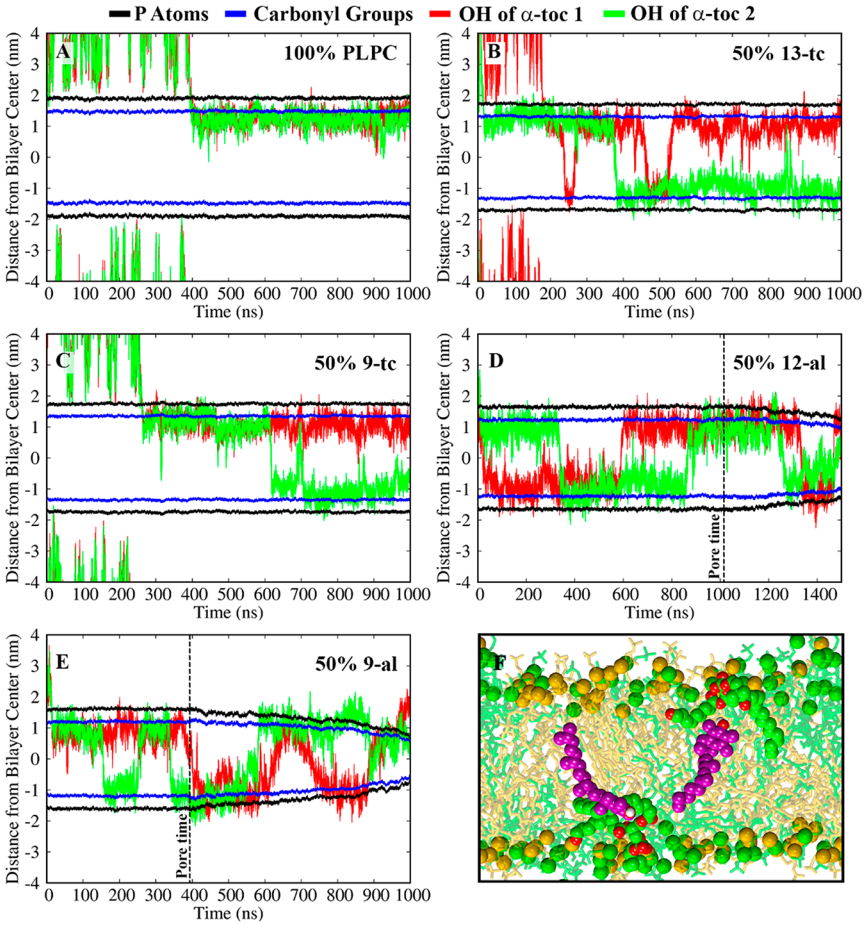

Figure 3. (A–E) Time evolution of the distance of α-toc's hydroxyl group from the bilayer center along the z-axis in nonoxidized and oxidized lipid bilayers containing two α-toc molecules. The dashed vertical lines show the times when pore formation first started to occur. Note that the definition of bilayer center becomes somewhat ambiguous during pore formation. (F) The preferred location of α-toc molecules inside the 50% 9-al bilayer is underneath the lipid carbonyl group. The color code for the lines is given on top of the picture.

probability for an α-toc to undergo flip-flop is higher in oxidized bilayers.

Flip-Flop Rate Calculation. To estimate the rate of α-toc flip-flops (k_{flip}), additional simulations with an α-toc initially at the bilayer center were performed. The initial configurations were taken from the z = 0 nm window in umbrella sampling simulations. Fifty independent simulations of each bilayer were independently run for 50 ns, and the time for the hydroxyl group of the α-toc to return from the bilayer center to the equilibrium position (t_d) was recorded. The rate of α-toc flip-flop across a lipid bilayer (k_{flip}) was calculated following the approach of Bennett et al.[42] using the equation

$$k_{flip} = \frac{1}{[(1/k_f) + (1/k_d)]} \times 1/2$$

where

$$k_f = k_d \times \exp(-\Delta G_{barrier}/RT)$$

and $k_d = t_d^{-1}$ where R and T are the gas constant and temperature, respectively. $\Delta G_{barrier}$ is the free-energy difference between the equilibrium position and the bilayer center. The half time for flip-flop ($t_{1/2}$) was calculated using[43]

$$t_{1/2} = \ln 2/k_{flip}$$

Table 3 shows the results and the parameters. The results show that α-toc molecules undergo rapid flip-flops especially in the aldehyde bilayers as compared to flip-flops in a pure phospholipid bilayer.

To put the results in Table 3 into context, we compare the α-toc flip-flop rates to those reported in different systems. In pure phospholipid bilayers, previous experimental studies have reported $t_{1/2}$ in a large unilamellar DPPC vesicle in the fluid phase (temperature range of 50–65 °C) to be in range from days to weeks, and no flip-flop was observed in the gel phase over 250 h.[44] Previous free-energy calculations[45] using umbrella sampling technique have suggested that the free-energy barrier for phospholipid flip-flop decreases upon increasing degree of oxidation in 1-palmitoyl-2-oleoyl-glycero-3-phosphocholine (POPC) bilayers, which indicates an increase in the lipid flip-flop rate. However, the flip-flop rates were not explicitly determined, and the free-energy barriers (between bilayer center and equilibrium position) remain relatively high, 65 ± 6 kJ/mol in the case of a 50% hydroperoxide bilayer.[45] Finally, in previous simulations, the phospholipid flip-flop rates in pure DPPC bilayers have been estimated to occur in time scales of 4–30 h.[46]

Next, we compare the α-toc flip-flop rates with those of cholesterol in different bilayers; it has been shown that cholesterol helps to protect membranes against oxidized lipids.[47,48] The flip-flop rates of cholesterol in pure DPPC bilayers range from 1.2×10^4 to 6.6×10^5 s^{-1}.[42] In unsaturated diarachidonyl-phosphocholine (DAPC, 20:4–20:4 phospho-

DOI: 10.1021/acs.jpcb.8b09064
J. Phys. Chem. B 2018, 122, 10362–10370

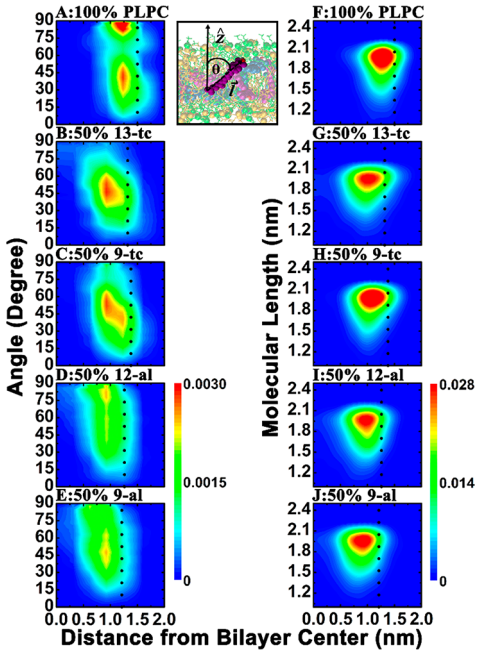

Figure 4. (A–E) Normalized two-dimensional histograms of α-toc's tilt angle in nonoxidized and oxidized bilayers containing 5.9% α-toc molecules. The hydroxyl group in the chromanol ring and the methyl group at the terminal chain represent head and tail of α-toc, respectively. The distance from head to tail of α-toc is defined as the molecular length ($\vec{l}$). (F–J) α-toc's molecular length is plotted as a function of the distance of α-toc's head from the bilayer center. (inset) The tilt angle is defined by the angle between the bilayer normal (z-axis) and the vector connecting the last methyl group in the tail to the hydroxyl group in the head of the α-toc molecule. The tilt angle of 0° represents α-toc oriented in parallel to the bilayer normal (z-axis), and 90° describes the α-toc being perpendicular to the bilayer normal. The dotted lines represent the average positions of the carbonyl groups in lipid chains.

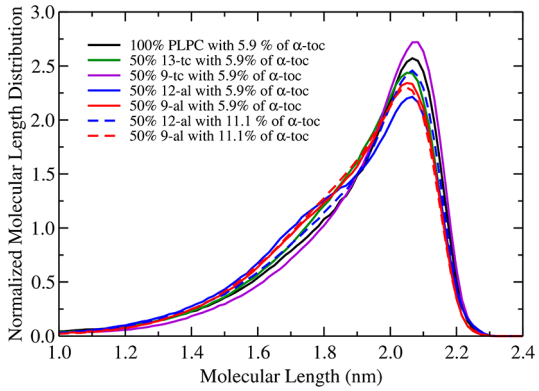

Figure 5. Distribution of α-toc's molecular length ($\vec{l}$) in oxidized and nonoxidized lipid bilayers containing 5.9% and 11.1% of α-toc molecules. The hydroxyl group in the chromanol ring and methyl group at the terminal chain represent head and tail of α-toc, respectively. The distance from head to tail of α-toc is defined the molecular length ($\vec{l}$).

choline (PC)) lipid bilayer, the flip-flop rates (5.2×10^5 to 3.7×10^6 s^{-1}) were observed to be an order of magnitude larger than in fully saturated DPPC lipid bilayers.[42,49] Our calculations show (Table 3) that the α-toc flip-flop rate and

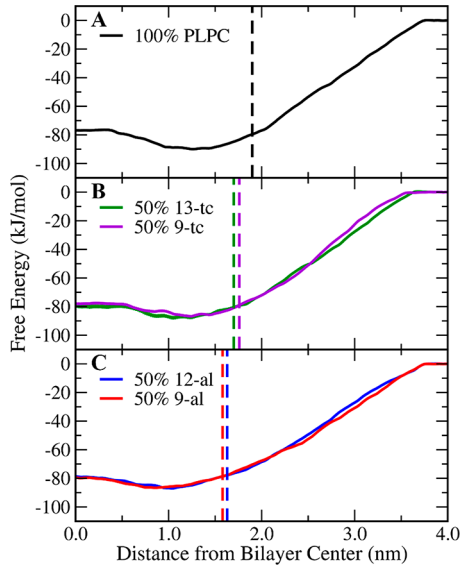

Figure 6. PMF for moving an α-toc from the center of a 100% PLPC bilayer (A), 50% hydroperoxide lipid (B), and a 50% aldehyde lipid (C) to the water phase as a function of distance in the z-direction from the bilayer center. The PMF in bulk water was set to zero. The dashed lines are the average positions of the phosphorus atoms in the lipid headgroup in each bilayer. The free energy of desorption (ΔG_{desorb}) is the difference in free energy between the equilibrium position and bulk water. The free-energy barrier ($\Delta G_{barrier}$) is the maximum free energy for α-toc to move from the equilibrium position to the bilayer center. All free-energy calculations in different lipid bilayers are listed in Table 2. The error in all systems is less than 1 kJ mol^{-1}.

Table 2. Equilibrium Positions Given as the Location of the α-toc Hydroxyl Group from the Bilayer Center[a]

systems	ΔG_{desorb} (kJ/mol)	$\Delta G_{barrier}$ (kJ/mol)	equilibrium position (nm)
100% PLPC	90.0 ± 0.7	13.5 ± 0.5	1.26 ± 0.01
50% 13-tc	87.8 ± 1.0	8.1 ± 0.5	1.10 ± 0.09
50% 9-tc	86.6 ± 0.7	9.2 ± 0.5	1.24 ± 0.02
50% 12-al	87.0 ± 0.7	8.3 ± 0.5	1.04 ± 0.02
50% 9-al	86.6 ± 0.5	7.1 ± 0.2	0.85 ± 0.01

[a] ΔG_{desorb} is the free energy of desorption, that is, the free-energy cost for moving an α-toc from its equilibrium position in bilayer into bulk water, and $\Delta G_{barrier}$ is the free energy for moving an α-toc from its equilibrium position to bilayer center. See also Figure 6.

the flip-flop half time in 100% PLPC bilayer are 4.2×10^5 s^{-1} and 1.65 μs, respectively. These values are consistent with a previous computational study using 1-stearoyl-2-docosahexaenoylphosphatidylcholine (SDPC, 18:0–22:6PC) and 1-stearoyl-2-oleoylphosphatidylcholine (SOPC, 18:0–18:1PC) bilayers.[16,50] From the binding free-energy calculations of α-toc with polyunsaturated phospholipids, the flip-flop rates have been estimated to be 7.5×10^5 s^{-1} and 2.5×10^5 s^{-1} in SDPC and SOPC lipid, respectively.[50] Here, for the oxidized lipid systems the flip-flop rates were found to be (all at 50%): 13-tc: 2.6×10^6 s^{-1}, 9-tc: 1.7×10^6 s^{-1}, 12-al: 5.7×10^6 s^{-1}, and 9-al: 6.4×10^6 s^{-1}. Thus, the flip-flop rates of α-toc in the oxidized bilayers are up to an order of magnitude larger than in the pure PLPC bilayer. This result suggests faster α-toc dynamics in oxidized lipid bilayer, thus providing a simple and robust mechanism to increase interactions with free radicals in membranes with oxidized lipids. We would also like to point

DOI: 10.1021/acs.jpcb.8b09064
J. Phys. Chem. B 2018, 122, 10362–10370

Table 3. Parameters[a] Associated with α-toc Flip-Flop Calculation in Different Lipid Bilayers

systems	t_d (ns)	k_d (s^{-1})	k_f (s^{-1})	k_{flip} (s^{-1})	average t_d (ns)	$\bar{k}_{flip}$ (s^{-1})	$t_{1/2}$ (μs)
100% PLPC	0.3−27.8	3.3×10^9 to 3.6×10^7	1.4×10^7 to 1.6×10^5	7.2×10^6 to 7.7×10^4	5.1 ± 5.8	4.2×10^5	1.65
50% 13-tc	0.1−21.8	1.0×10^{10} to 4.6×10^7	3.8×10^8 to 1.7×10^6	1.8×10^8 to 8.4×10^5	7.1 ± 5.1	2.6×10^6	0.27
50% 9-tc	0.5−27.7	2.0×10^9 to 3.6×10^7	4.9×10^7 to 8.8×10^5	2.4×10^7 to 4.3×10^5	7.1 ± 5.9	1.7×10^6	0.41
50% 12-al	0.1−9.0	1.0×10^{10} to 1.1×10^8	3.5×10^8 to 3.9×10^6	1.7×10^8 to 1.9×10^6	3.0 ± 2.4	5.7×10^6	0.12
50% 9-al	0.4−12.0	2.5×10^9 to 8.3×10^7	1.4×10^8 to 4.8×10^6	6.7×10^7 to 2.2×10^6	4.2 ± 2.8	6.4×10^6	0.11
100% SDPC[b]	8−55	1.3×10^8 to 1.8×10^7	5.7×10^6 to 8.3×10^5	2.7×10^6 to 4.0×10^5		7.5×10^5	0.92
100% SOPC[b]	8−60	1.3×10^8 to 1.7×10^7	2.2×10^6 to 2.9×10^5	1.1×10^6 to 1.4×10^5		2.5×10^5	2.77

[a]Note: t_d is the time for the α-toc's hydroxyl group to move from the bilayer center to the equilibrium position in the bilayer. k_d is the rate for an α-toc to move from the center of bilayer to the equilibrium position; k_d was estimated by $k_d = t_d^{-1}$. k_f is the rate for an α-toc to move from equilibrium to the bilayer center and was calculated by $k_f = k_d \times \exp(-\nabla G_{barrier}/RT)$. The rate of α-toc flip-flop (k_{flip}) was calculated by $k_{flip} = \frac{1}{[(1/k_f) + (1/k_d)]} \times 1/2$. The haft time for α-toc flip-flop ($t_{1/2}$) was calculated by $t_{1/2} = \ln 2/k_{flip}$. [b]Data were taken from a previous study by Leng et al.[50]

out that pore formation in the absence of external fields is a stochastic process, and hence the pore formation times in Table 1 should not be taken as absolute values. Providing a reasonably accurate estimate with small error bars would, however, require a very large number of independent simulations and is beyond the scope of the current study. It is possible to induce pore formation using an electric field, which can be used to overcome the energy barriers as has been demonstrated by Yusupov et al.[51] The review by Gurtovenko et al.[52] provides a good discussion of flip-flop and pore formation via different mechanisms.

CONCLUSION

We have performed a series of MD simulations of α-toc in different oxidized and nonoxidized lipid bilayers to better understand the role of α-toc in oxidative stress. The presence of ∼11% of α-toc was confirmed to stabilize oxidized membranes and prevent water pore formation in a long simulation times over 5 μs. We investigated the locations and conformations of α-toc both in oxidized and nonoxidized bilayers. The results show that α-toc's hydroxyl group favors staying at the bilayer interface for both cases. In addition, α-toc was observed flip-flopping in both oxidized and nonoxidized lipid bilayers. We calculated the free-energy profiles to obtain the free-energy barrier and to estimate the α-toc flip-flop rate in the different bilayers. Importantly, our results show that the free-energy barriers for α-toc flip-flop become significantly suppressed in the presence of oxidized lipids. As a consequence, the flip-flop rate increases with lipid peroxidation by up to an order of magnitude compared to the pure PLPC bilayer. The rate increases in the following order: aldehyde > hydroperoxide > PLPC. This significantly increased flip-flop rate provides a physical mechanism that allows α-toc to scavenge radicals to protect membranes from oxidative attack and to help stabilize membrane under oxidative stress.

Our results indicate that α-toc flip-flop may indeed be essential for membrane protection. To elaborate its role, it would be interesting to investigate its kinetics in multicomponent membranes containing polyunsaturated lipids and in the presence of cholesterol. Such studies would help answer questions about synergistic effects of cholesterol and α-toc, possible aggregation behaviors, and the locations, both vertical and lateral, of both oxidized lipids and α-toc. Finally, we would also like to point out that there are several interesting issues related to interactions of oxidized lipids with the lipid matrix including the length of the chains and, in particular, how oxidized lipids modify the energy barriers for different types of small molecules.[53]

ASSOCIATED CONTENT

Supporting Information

The Supporting Information is available free of charge on the ACS Publications website at DOI: 10.1021/acs.jpcb.8b09064.

Abbreviations of molecular names, distribution of α-toc's tilt angle in nonoxidized/oxidized lipid bilayers containing 5.9% and 11.1% of α-toc molecules, distribution of α-toc's tilt angle with respect to the bilayer normal (z-axis) in nonoxidized and oxidized lipid bilayers, and normalized two-dimensional histogram of α-toc's molecular length as a function of its tilt angle in nonoxidized and oxidized bilayers containing 5.9% α-toc molecules (PDF)

AUTHOR INFORMATION

Corresponding Authors

*E-mail: jirasak.w@ku.ac.th. (J.W.)
*E-mail: mkarttu@uwo.ca. (M.K.)

ORCID

Mikko Karttunen: 0000-0002-8626-3033

Notes

The authors declare no competing financial interest.

ACKNOWLEDGMENTS

This work was financially supported by Kasetsart Univ. Research and Development Institute and Faculty of Science at Kasetsart Univ. (J.W.). The support of the Thailand Research Fund (TRF) through the Royal Golden Jubilee Ph.D. Program (Grant No. PHD/0204/2559) and the TRF Research Scholar Program (Grant No. RSA6180021) for P.B. and J.W., respectively, is acknowledged. M.K. would like to thank the Natural Sciences and Engineering Research Council of Canada and the Canada Research Chairs Program. Computing facilities have been provided by SHARCNET (www.sharcnet.ca), Compute Canada (www.computecanada.ca), and the Department of Physics, Faculty of Science, Kasetsart Univ.

REFERENCES

(1) Burton, G. J.; Jauniaux, E. Oxidative stress. *Best Pract. Res. Clin. Obstet. Gynaecol.* **2011**, *25*, 287−299.

(2) Atkinson, J.; Epand, R. F.; Epand, R. M. Tocopherols and tocotrienols in membranes: A critical review. *Free Radical Biol. Med.* **2008**, *44*, 739−764.

DOI: 10.1021/acs.jpcb.8b09064
J. Phys. Chem. B 2018, 122, 10362−10370

(3) Raederstorff, D.; Wyss, A.; Calder, P. C.; Weber, P.; Eggersdorfer, M. Vitamin E function and requirements in relation to PUFA. *Br. J. Nutr.* **2015**, *114*, 1113−1122.
(4) Podda, M.; Weber, C.; Traber, M. G.; Packer, L. Simultaneous determination of tissue tocopherols, tocotrienols, ubiquinols, and ubiquinones. *J. Lipid Res.* **1996**, *37*, 893−901.
(5) Niki, E. Role of vitamin E as a lipid-soluble peroxyl radical scavenger: In vitro and in vivo evidence. *Free Radical Biol. Med.* **2014**, *66*, 3−12.
(6) Burton, G. W.; Joyce, A.; Ingold, K. U. First proof that vitamin E is major lipid-soluble, chain-breaking antioxidant in human blood plasma. *Lancet* **1982**, *320*, 327.
(7) Burton, G. W. Vitamin E: Molecular and biological function. *Proc. Nutr. Soc.* **1994**, *53*, 251−262.
(8) Atkinson, J.; Harroun, T.; Wassall, S. R.; Stillwell, W.; Katsaras, J. The location and behavior of alpha-tocopherol in membranes. *Mol. Nutr. Food Res.* **2010**, *54*, 641−651.
(9) Ausili, A.; de Godos, A. M.; Torrecillas, A.; Aranda, F. J.; Corbalan-Garcia, S.; Gomez-Fernandez, J. C. The vertical location of alpha-tocopherol in phosphatidylcholine membranes is not altered as a function of the degree of unsaturation of the fatty acyl chains. *Phys. Chem. Chem. Phys.* **2017**, *19*, 6731−6742.
(10) Qin, S. S.; Yu, Z. W.; Yu, Y. X. Structural and kinetic properties of alpha-tocopherol in phospholipid bilayers, a molecular dynamics simulation study. *J. Phys. Chem. B* **2009**, *113*, 16537−16546.
(11) Qin, S. S.; Yu, Z. W. Molecular dynamics simulations of alpha-tocopherol in model biomembranes. *Acta Phys.-Chim. Sin.* **2011**, *27*, 213−227.
(12) Marquardt, D.; Williams, J. A.; Kucerka, N.; Atkinson, J.; Wassall, S. R.; Katsaras, J.; Harroun, T. A. Tocopherol activity correlates with its location in a membrane: A new perspective on the antioxidant vitamin E. *J. Am. Chem. Soc.* **2013**, *135*, 7523−7533.
(13) Marquardt, D.; Williams, J. A.; Kinnun, J. J.; Kucerka, N.; Atkinson, J.; Wassall, S. R.; Katsaras, J.; Harroun, T. A. Dimyristoyl phosphatidylcholine: A remarkable exception to α-tocopherol's membrane presence. *J. Am. Chem. Soc.* **2014**, *136*, 203−210.
(14) Marquardt, D.; Kučerka, N.; Katsaras, J.; Harroun, T. A. α-tocopherol's location in membranes is not affected by their composition. *Langmuir* **2015**, *31*, 4464−4472.
(15) Cordeiro, R. M. Reactive oxygen species at phospholipid bilayers: Distribution, mobility and permeation. *Biochim. Biophys. Acta, Biomembr.* **2014**, *1838*, 438−444.
(16) Leng, X. L.; Kinnun, J. J.; Marquardt, D.; Ghefli, M.; Kucerka, N.; Katsaras, J.; Atkinson, J.; Harroun, T. A.; Feller, S. E.; Wassall, S. R. Alpha-tocopherol is well designed to protect polyunsaturated phospholipids: MD simulations. *Biophys. J.* **2015**, *109*, 1608−1618.
(17) Sharma, V. K.; Mamontov, E.; Tyagi, M.; Urban, V. S. Effect of alpha-tocopherol on the microscopic dynamics of dimyristoylphosphatidylcholine membrane. *J. Phys. Chem. B* **2016**, *120*, 154−163.
(18) Boonnoy, P.; Karttunen, M.; Wong-ekkabut, J. Alpha-tocopherol inhibits pore formation in oxidized bilayers. *Phys. Chem. Chem. Phys.* **2017**, *19*, 5699−5704.
(19) Ausili, A.; Torrecillas, A.; de Godos, A. M.; Corbalan-Garcia, S.; Gomez-Fernandez, J. C. Phenolic group of alpha-tocopherol anchors at the lipid-water interface of fully saturated membranes. *Langmuir* **2018**, *34*, 3336−3348.
(20) Berendsen, H. J. C.; Postma, J. P. M.; van Gunsteren, W. F.; Hermans, J. Interaction models for water in relation to protein hydration. In *Intermolecular Forces;* Pullman, B., Ed.; D. Reidel: Dordrecht, The Netherlands, 1981; pp 331−342.
(21) Bachar, M.; Brunelle, P.; Tieleman, D. P.; Rauk, A. Molecular dynamics simulation of a polyunsaturated lipid bilayer susceptible to lipid peroxidation. *J. Phys. Chem. B* **2004**, *108*, 7170−7179.
(22) Wong-ekkabut, J.; Xu, Z.; Triampo, W.; Tang, I. M.; Peter Tieleman, D.; Monticelli, L. Effect of lipid peroxidation on the properties of lipid bilayers: A molecular dynamics study. *Biophys. J.* **2007**, *93*, 4225−4236.
(23) Boonnoy, P.; Jarerattanachat, V.; Karttunen, M.; Wong-ekkabut, J. Bilayer deformation, pores, and micellation induced by oxidized lipids. *J. Phys. Chem. Lett.* **2015**, *6*, 4884−4888.
(24) Abraham, M. J.; Murtola, T.; Schulz, R.; Páll, S.; Smith, J. C.; Hess, B.; Lindahl, E. GROMACS: High performance molecular simulations through multi-level parallelism from laptops to supercomputers. *SoftwareX* **2015**, *1*, 19−25.
(25) Bussi, G.; Donadio, D.; Parrinello, M. Canonical sampling through velocity rescaling. *J. Chem. Phys.* **2007**, *126*, 014101.
(26) Parrinello, M.; Rahman, A. Polymorphic transitions in single crystals: A new molecular dynamics method. *J. Appl. Phys.* **1981**, *52*, 7182−7190.
(27) Darden, T.; York, D.; Pedersen, L. Particle mesh Ewald: An N.Log(N) method for Ewald sums in large systems. *J. Chem. Phys.* **1993**, *98*, 10089−10092.
(28) Essmann, U.; Perera, L.; Berkowitz, M. L.; Darden, T.; Lee, H.; Pedersen, L. G. A smooth particle mesh Ewald method. *J. Chem. Phys.* **1995**, *103*, 8577−8593.
(29) Karttunen, M.; Rottler, J.; Vattulainen, I.; Sagui, C. Electrostatics in biomolecular simulations: Where are we now and where are we heading? *Curr. Top. Membr.* **2008**, *60*, 49−89.
(30) Hess. P-LINCS: A parallel linear constraint solver for molecular simulation. *J. Chem. Theory Comput.* **2008**, *4*, 116−122.
(31) Wong-ekkabut, J.; Karttunen, M. Assessment of common simulation protocols for simulations of nanopores, membrane proteins, and channels. *J. Chem. Theory Comput.* **2012**, *8*, 2905−2911.
(32) Wong-ekkabut, J.; Karttunen, M. The good, the bad and the user in soft matter simulations. *Biochim. Biophys. Acta, Biomembr.* **2016**, *1858*, 2529−2538.
(33) Khuntawee, W.; Karttunen, M.; Wong-ekkabut, J. A molecular dynamics study of conformations of beta-cyclodextrin and its eight derivatives in four different solvents. *Phys. Chem. Chem. Phys.* **2017**, *19*, 24219−24229.
(34) Humphrey, W.; Dalke, A.; Schulten, K. VMD: Visual molecular dynamics. *J. Mol. Graphics* **1996**, *14*, 33−8.
(35) Torrie, G. M.; Valleau, J. P. Nonphysical sampling distributions in Monte Carlo free-energy estimation: Umbrella sampling. *J. Comput. Phys.* **1977**, *23*, 187−199.
(36) Kumar, S.; Rosenberg, J. M.; Bouzida, D.; Swendsen, R. H.; Kollman, P. A. The weighted histogram analysis method for free-energy calculations on biomolecules. I. The method. *J. Comput. Chem.* **1992**, *13*, 1011−1021.
(37) Hub, J. S.; Winkler, F. K.; Merrick, M.; de Groot, B. L. Potentials of mean force and permeabilities for carbon dioxide, ammonia, and water flux across a Rhesus protein channel and lipid membranes. *J. Am. Chem. Soc.* **2010**, *132*, 13251−13263.
(38) Howard, A. C.; McNeil, A. K.; McNeil, P. L. Promotion of plasma membrane repair by vitamin E. *Nat. Commun.* **2011**, *2*, 597.
(39) Rog, T.; Stimson, L. M.; Pasenkiewicz-Gierula, M.; Vattulainen, I.; Karttunen, M. Replacing the cholesterol hydroxyl group with the ketone group facilitates sterol flip-flop and promotes membrane fluidity. *J. Phys. Chem. B* **2008**, *112*, 1946−1952.
(40) Gurtovenko, A. A.; Vattulainen, I. Molecular mechanism for lipid flip-flops. *J. Phys. Chem. B* **2007**, *111*, 13554−13559.
(41) Sapay, N.; Bennett, W. F. D.; Tieleman, D. P. Thermodynamics of flip-flop and desorption for a systematic series of phosphatidylcholine lipids. *Soft Matter* **2009**, *5*, 3295−3302.
(42) Bennett, W. F. D.; MacCallum, J. L.; Hinner, M. J.; Marrink, S. J.; Tieleman, D. P. Molecular view of cholesterol flip-flop and chemical potential in different membrane environments. *J. Am. Chem. Soc.* **2009**, *131*, 12714−12720.
(43) Bennett, W. F. D.; Tieleman, D. P. Molecular simulation of rapid translocation of cholesterol, diacylglycerol, and ceramide in model raft and nonraft membranes. *J. Lipid Res.* **2012**, *53*, 421−429.
(44) Marquardt, D.; Heberle, F. A.; Miti, T.; Eicher, B.; London, E.; Katsaras, J.; Pabst, G. H-1 NMR shows slow phospholipid flip-flop in gel and fluid bilayers. *Langmuir* **2017**, *33*, 3731−3741.
(45) Razzokov, J.; Yusupov, M.; Vanuytsel, S.; Neyts, E. C.; Bogaerts, A. Phosphatidylserine induced by oxidation of the plasma

DOI: 10.1021/acs.jpcb.8b09064
J. Phys. Chem. B 2018, 122, 10362−10370

membrane: A better insight by atomic scale modeling. *Plasma Processes Polym.* **2017**, *14*, 1700013.
(46) Bennett, W. F. D.; MacCallum, J. L.; Tieleman, D. P. Thermodynamic analysis of the effect of cholesterol on dipalmitoylphosphatidylcholine lipid membranes. *J. Am. Chem. Soc.* **2009**, *131*, 1972−1978.
(47) Khandelia, H.; Loubet, B.; Olżyńska, A.; Jurkiewicz, P.; Hof, M. Pairing of cholesterol with oxidized phospholipid species in lipid bilayers. *Soft Matter* **2014**, *10*, 639−647.
(48) Owen, M. C.; Kulig, W.; Rog, T.; Vattulainen, I.; Strodel, B. Cholesterol protects the oxidized lipid bilayer from water injury: An all-atom molecular dynamics study. *J. Membr. Biol.* **2018**, *251*, 521−534.
(49) Neuvonen, M.; Manna, M.; Mokkila, S.; Javanainen, M.; Rog, T.; Liu, Z.; Bittman, R.; Vattulainen, I.; Ikonen, E. Enzymatic oxidation of cholesterol: Properties and functional effects of cholestenone in cell membranes. *PLoS One* **2014**, *9*, e103743.
(50) Leng, X.; Zhu, F.; Wassall, S. R. Vitamin E has reduced affinity for a polyunsaturated phospholipid: An umbrella sampling molecular dynamics simulations study. *J. Phys. Chem. B* **2018**, *122*, 8351−8358.
(51) Yusupov, M.; Van der Paal, J.; Neyts, E. C.; Bogaerts, A. Synergistic effect of electric field and lipid oxidation on the permeability of cell membranes. *Biochim. Biophys. Acta, Gen. Subj.* **2017**, *1861*, 839−847.
(52) Gurtovenko, A. A.; Anwar, J.; Vattulainen, I. Defect-mediated trafficking across cell membranes: Insights from in silico modeling. *Chem. Rev.* **2010**, *110*, 6077−6103.
(53) Razzokov, J.; Yusupov, M.; Cordeiro, R. M.; Bogaerts, A. Atomic scale understanding of the permeation of plasma species across native and oxidized membranes. *J. Phys. D: Appl. Phys.* **2018**, *51*, 365203.

DOI: 10.1021/acs.jpcb.8b09064
J. Phys. Chem. B 2018, 122, 10362−10370